

Experimental Tomographic Scanning (TOSCA) Imagers

H. Hovland,

Norwegian Defence Research Establishment (FFI), P. O. Box 25, N-2027 Kjeller, Norway
harald.hovland@ffi.no; phone (+47) 6380 7312; fax (+47) 6380 7212

ABSTRACT

The tomographic scanner (TOSCA) detects signals using line detectors scanning a scene at regularly distributed angles. These line scan signals are then processed to reconstruct 2-dimensional images. In the simplest form, a 1-axis rotating conical scan optics scans across a simple patterned reticle, the signal collection being done with a single pixel detector. Experimental mono- and multispectral cameras using this approach are demonstrated under varying illumination conditions. Of particular interest is the TOSCA system's ability to handle and compensate for light sources modulated with a frequency higher than that of the frame rate. We also demonstrate for the first time a TOSCA imager operating in the infrared region. The device is put together using 3D-printed key parts and low cost optical components, leading to a very economical infrared camera.

Keywords: Tomography, tomographic image processing, imaging systems, infrared imaging, image reconstruction techniques, Fourier optics and signal processing.

1. INTRODUCTION

Tomography, from Greek *tomos* (slice), is a means for reconstructing higher dimensional signals from a collection of projections. The technique itself was invented and published back in 1917 by Radon^[1], but became famous through Hounsfield's invention of the CAT scanner^[2], which earned him a Nobel prize in 1972. When x-rays are radiated through the body, it is not possible to directly determine at which point along the path the radiation is absorbed, but it is possible to measure the total radiation loss along the path. Several such measurements are made using measurements from parallel beams to obtain a cross section across the body in one direction. By making similar measurements in different directions, corresponding cross sections in different orientations can be built up. The information thus obtained can be used to reconstruct a 2-dimensional image of the absorption.

With increasing computational capability, newer approaches have been made where scattering is modeled to handle both acoustic and optical waves in strongly scattering media, and most papers on optical tomography deals with this kind of scenarios. The TOSCA concept, however, is much more similar to the parallel beam X-ray case. Here, the detection process is achieved with one or several line detectors scanning the scene. A line detector is here understood either as a detector whose active area has the shape of a thin line, or that the light passes a thin slit before hitting the detector.

The TOSCA camera concept was first presented and then demonstrated in the visible band by the author^[3,4]. In this work we show that the TOSCA concept is capable of handling very rapidly varying scene illumination. We also demonstrate for the first time a TOSCA camera operating in the infrared spectral range. Of special interest is the fact that most of the camera was printed using a 3D-printer, and the optics are low cost, making the system relatively affordable.

In this paper, a simplified presentation of the TOSCA process is explained, before experimental setup and results are presented. Of particular interest is the TOSCA system's ability to handle and compensate for modulated light sources with a modulation frequency higher than the frame rate.

2. THEORY

The basic principles behind and the background leading up to the TOSCA detection process is described in previous publications^[3, 4, 5, 6, 7], including the mathematics and noise processes, so this chapter is intended to serve as a simplified introduction to the theory. In the simplest case, the line detector scans across an image of the scene, the latter being restricted by an aperture. The scans are done at regularly distributed angles relative to the image of the scene. In this way, each scan represents a plane wave in a specific direction given by the normal to the line detector orientation. All

information about spatial plane waves in one direction can be represented as amplitude and phase along a line crossing the origin in Fourier space. The Fourier transform of the scan signal can therefore be used to fill out a line in the Fourier space representation of the scene. In principle, making several scans with different orientations can thus be used to fill out the information about the Fourier space representation of the scene. In principle, once all information about the Fourier space of the scene is known, an inverse transform can be performed to reconstruct the scene.

There are several issues with this approach. First, the discrete nature of the sampling means a discrete number of points will be obtained in Fourier space. Second, the angular density of points in Fourier space decreases with increasing distance from the origin. Notably, the origin is determined several times during the recording of one frame, once per angular scan. Third, the representation in the Fourier domain obtained in the TOSCA measurement process is done in polar co-ordinates, whereas the traditional transforms between frequency (Fourier) and spatial representation are done between sets of Cartesian co-ordinates. And, finally, there are a limited number of samples per scan, meaning that the cyclic properties of the Fourier transform could affect the results.

To take the last issue first, zero-padding the spatial signals before the Fourier transform limits the effect of the cyclic boundary conditions^[8]. After filtering and transforming back to the spatial domain, the signal is then truncated.

As for all sampling, artifacts will appear if the sampling relative to the Nyquist criterion is not sufficient^[9]. In the TOSCA reconstruction, insufficient angular sampling typically takes the shape of radiating lines away from hot spots at a certain distance, but the artifacts will typically not severely affect structures in close proximity to the hot spot.

The transform between polar and Cartesian coordinates in Fourier space represents an important issue. The coupling between frequency components during an interpolation process in the Fourier domain can significantly affect the results in the spatial domain. The filtered back projection process introduced by Bracewell and Riddle^[10] has been found to avoid the coordinate transform interpolation in the Fourier domain altogether, and is also both memory and computationally efficient. In the filtered back projection approach, a transform of each line scan to Fourier space is followed by a multiplication of each frequency component with its distance from the origin. An exception is done at the origin, where the factor is not 0, but $\frac{1}{4}$ of the smallest nonzero frequency value to account for the discrete nature of the sampling^[3]. If needed in the specific application, additional smoothing coefficients are also included in this process. After this filtering, the result is brought back to the spatial domain by an inverse Fourier transform. The resulting filtered signal is then projected onto a Cartesian grid, where each grid point is assigned the value of its projection onto the filtered scan line, typically using linear interpolation. Summing up the resulting plane waves in different directions, one for each angular scan, finalizes the reconstruction.

3. EXPERIMENTS

3.1 Visible single color operation

The first experimental TOSCA demonstrator^[4] was based on the theoretical concepts in previous work^[3]. A sketch of the first demonstrator system is shown in Figure 1. A focusing lens, followed a pair of flat mirrors were used to project an image of the scene onto a fixed reticle with 65 radially oriented slits. While the lens and mirror pair rotates, the reticle remains stationary, and the scene is scanned across the reticle slits sequentially. A circular aperture, rotating with the mirrors and lens, limits the field of view. Behind the reticle, the transmitted light is brought back to the rotational axis using a pair of mirrors, and collimated by another lens before being collected by the lens/detector assembly.

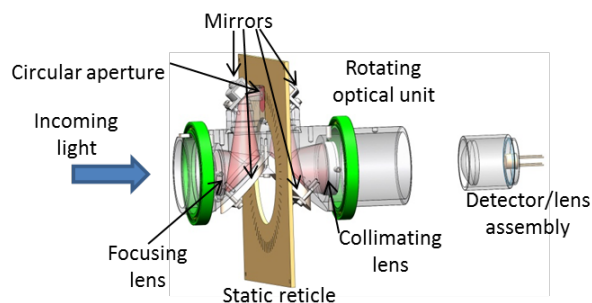


Figure 1. Sketch of the TOSCA configuration used in the first experimental setup.

A characterization of the point spread function is shown in Figure 2. A homogeneous background is created by reflecting sunlight off plain copying paper, and a point is created by reflecting a laser source off the paper at different positions.

To demonstrate the imaging capabilities, an image from the first ever TOSCA recording is shown in Figure 3. Sun light was illuminating the scene indirectly, to obtain stable light intensity as a function of time. This image is part of a 12 Hz image frame video recording.

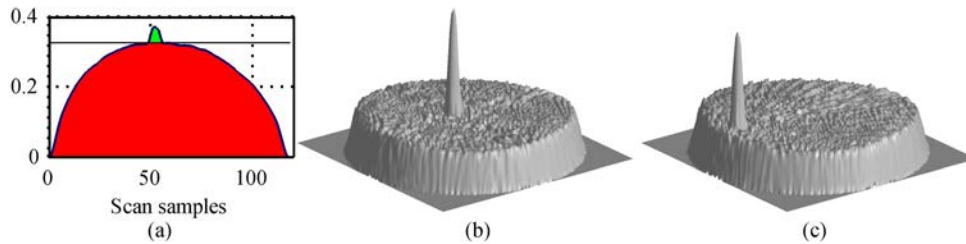


Figure 2. (a) Laser spot (green) and sun (red) reflection contributions in a single scan. Reconstructed images with (b) centered and (c) de-centered laser spots. Images from Hovland^[4].



Figure 3. Imaging properties demonstrated during the first ever recording with the TOSCA demonstrator, showing the author looking into the camera lens.

3.2 Compensation of illumination modulation with frequency components higher than the frame rate

An interesting property of the system appears when using artificial illumination. In Norway, indoors illumination using fluorescent lamps have a significant 100 Hz modulation frequency, almost an order of magnitude higher than the 12 Hz frame rate. This is shown in Figure 4 (a), where the illumination variation, measured to be around 20-30 % of the average level, is not compensated for, giving the hair of the subject an almost wavy look. Despite the high modulation frequency, it is nevertheless possible to compensate for this. The reason is that the total intensity is recorded for each angular scan, at the much higher rate of 780 Hz. The determination of the intensity at each line scan is inherent in the processing, and it is therefore possible to both detect and characterize the intensity modulation, and to compensate for it using a simple normalization. The result is shown in Figure 4 (b), where the hair no longer shows the wavy feature.

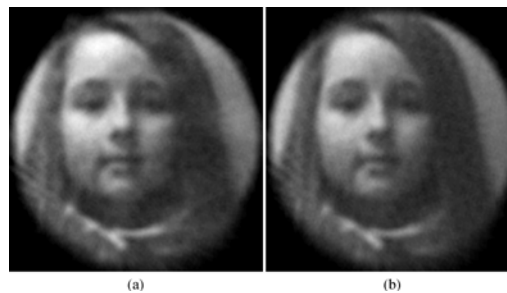


Figure 4. (a) “Victoria”, recorded using artificial illumination, featuring 100 Hz modulation, much a frequency much higher than the 12 Hz frame rate. The apparent waviness of the hair is an artifact of this illumination modulation. (b) “Victoria”, image, where the illumination modulation level has been determined from the recordings and compensated for, by determining the intensity at each line scan.

3.3 Multi-spectral operation

To demonstrate multispectral operation, a Thorlabs FD2G green interference filter was used as a 45° spectral beam-splitter after the collimator lens shown in Figure 1. The two resulting light beams were then collected using two (identical) lens/detector assemblies. The modified setup is shown in Figure 5 (a).

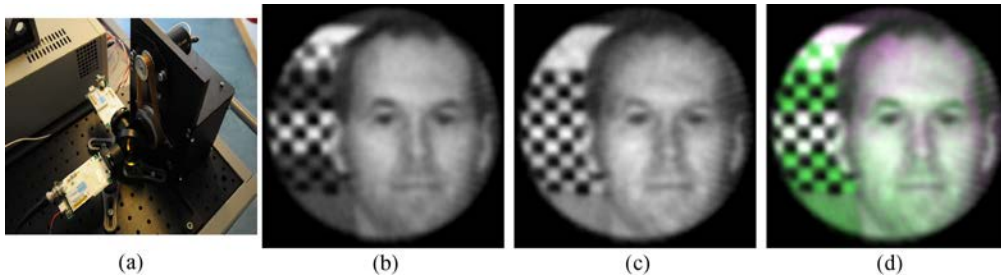


Figure 5. (a) Multispectral TOSCA setup. A spectral interference filter splits the beam in two. Each beam is detected with a lens/detector pair. (b)-(d) Author image with green/white, green/ black and white/black checkerboard patterns in (b) 'non-green' channel, (c) 'green' channel and (d) a color-coded combined image. The white/black checkerboard pattern transition color purity is due to perfect alignment between channels, inherent in the TOSCA system. Images from Hovland^[4].

Operation was modified by changing the recording from one detector channel to two. The resulting images from the 'non-green' and 'green' channels are presented in Figure 5 (b) and (c), respectively, and a composite two-channel image is shown in (d). The black/white pattern is of particular interest. Both 'non-green' and 'green' dominance is visible elsewhere, but does not appear in any black/white transition. Color artifacts often appear at such transitions in multispectral images from cameras with spectral misalignment, and can cause problems when looking for objects with a specific spectral signature or during anomaly detection, particularly when looking for sub-pixel targets^[11]. In the TOSCA camera this problem is different, as the image geometry is defined by the narrow reticle slits and the aperture, which are common for all spectral components. Similar artifacts might instead appear if the detector/amplifier chains of different spectral channels have different temporal filter or non-linear characteristics. In addition, artifacts due to the point spread function could also affect this issue, as the color of a strong intensity peak would create surrounding ripples.

3.4 Infrared TOSCA

An infrared (IR) TOSCA-demonstrator setup has been built. The setup is very similar to Figure 1, except that the focusing and collimating lenses no longer rotate with the mirrors and circular aperture. The main components (except the motor, drive belt, roller bearings, optics and detector assemblies) were printed on a Makerbot Replicator 2X using ABS plastic. The focusing and collimating lenses were Thorlabs best form 75 mm focal length, 1" diameter uncoated BK-7 lenses, whereas the collecting optics in front of the detector consisted of a Thorlabs 40 mm focal length, 1" diameter BK-7 best form lens. The detector used was a 3 mm × 3 mm Thorlabs PDA30G-EC PbS detector. A Umicore germanium substrate was used just in front of the detector as a 1.8 μm long-pass filter. Given the transmission curves of the BK-7 lenses, the germanium filter and the PbS detector responsivity, the overall system spectral responsivity should be in the 1.8-2.5 μm range, although this has not been confirmed by measurements.



Figure 6. IR TOSCA reticle, printed with the 3D printer. The reticle incorporates the fixture frame with mounting holes leading to an automatic centering of the mask. As seen, not all the 21-slot air gaps are open, so a grinding process was necessary to produce acceptable slits. A simple hand tool was found sufficient.

The reticle, shown in Figure 6, was also 3D-printed using ABS plastic used 21 air gap slits with a designed 0.6 mm slit width, for a slightly less than 6 mm diameter circular aperture (which would nominally result in a 10 pixel wide scene).

This proved to be too demanding for the printer, but acceptable results were obtained using a hand tool to grind the slits after printout. Slots into which the 1.3 mm aluminum first surface mirrors could be inserted proved to be of acceptable accuracy, also in terms of parallelism, and the mirrors were simply pushed in place with only minor adjustments being necessary. The adjustments were made using paper in some locations on the mirror back sides. When the optical unit was rotated slowly around its axis prior to mounting the lenses, a small movement was observed when looking along the rotational axis, but the rotating aperture was observed to move together with the scene, which would indicate a sufficient alignment, provided the detector/lens assembly field of view is sufficient to cover the whole reticle.

The IR TOSCA setup did not include a reference sensor to determine absolute orientation, so the target orientation had to be determined during post processing. Once aligned, it retained the alignment throughout a recording, though, even if the motor speed was only stabilized in a stand-alone circuit. One of the reasons is that the reconstruction algorithms feature minimum signal detection, corresponding to the time when no reticle slits overlap the circular aperture between each line scan. By tracking the temporal location of these minimum signals, and then resampling the line scan between consecutive minima, it is possible to compensate for both offset and slowly varying scan speeds. This has the advantage that no particular control loop is strictly required for the motor steering, as inertia limits the speed variations within the millisecond time span between detection minima.

The lenses were put in place using simple press fit fixtures consisting of three small half-cylinder shapes in a circular hole slightly larger than the lens diameter. Ball bearings were press-fitted onto the spinning optical unit. The optical unit was made in two parts, fixed together using four screws. The ball bearings were press-fitted inside fixtures that also held the lenses on each side, and the lens/detector assembly was press-fitted inside a unit that also held the collimator lens.

The motor used was a SmartMotor, from Moog Animatics. The detector signals were recorded using a National Instruments NI PCI-6123 A/D-card. Sampling was done at 100 kHz prior to digital low-pass filtering and resampling.

The complete assembly is shown in Figure 7.



Figure 7. IR TOSCA camera, seen from two angles. The unit consists of, from left to right: Lens holder (red), roller bearing fixture (black), roller bearing (steel), periscopic mirror holder with circular aperture (black, circular barrel), 21-slot air gap reticle (black rounded square shape), motor fixture with motor (black), periscopic mirror holder with toothed wheel incorporated (black, connected to the motor toothed wheel), roller bearing (steel), collimator lens holder with press fit tube for lens/detector assembly (red), detector/lens assembly (black).

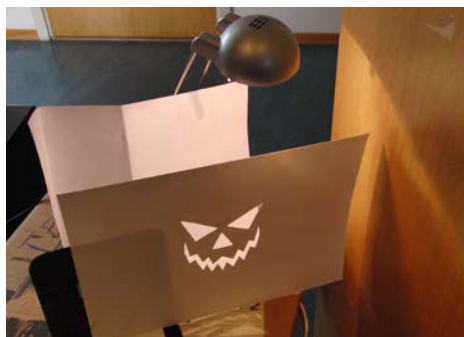


Figure 8. Halloween target mask used for the IR TOSCA experiment.

The target, shown in Figure 8, was made as a Halloween cardboard mask. At the back of the cardboard mask, plain white copying paper was illuminated using a halogen lamp to create a (relatively) uniform target.

The IR TOSCA camera was operated at a 5 Hz frame rate. A sample reconstruction is shown in Figure 9. As can be seen, the target is relatively easy to recognize, despite the inherently low sampling and relatively crude optics. The image was observed to move and degrade somewhat during the recording; this is partly due to camera motion, partly to the 100 Hz modulation of the Halogen lamp, which in this case was close to the 105 Hz line scan frequency.

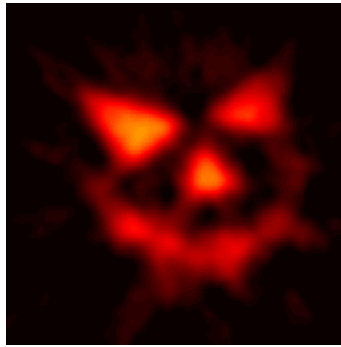


Figure 9. Halloween target mask reconstruction. The camera operated at 5 Hz, and the 21 slit reticle had a 0.6 mm slit width. In combination with the 6 mm circular aperture, this would indicate a nominal 10x10 pixel resolution.

4. CONCLUSIONS

The TOSCA imager has been demonstrated in both the visible and the infrared band. It has been shown that practical systems can be created, and due to its special scanning properties it is found capable to handle significant illumination modulation at frequencies far higher than the sampling rate. The use of a relatively low cost 3D-printer has proven to be sufficient to create a very low cost infrared camera, where a PC would represent the most significant cost component. The motor used in the setup could be replaced with a cheaper unregulated unit, and the A/D card could be replaced by the sound card input of a regular PC, making IR imaging accessible on a limited budget.

ACKNOWLEDGEMENTS

The author is grateful to Prof. S E Hamran, Dr. T Skauli and Dr. J Moen for helpful discussions during this work.

REFERENCES

- [1] Radon, J., "Über die Bestimmung von Funktionen durch ihre Integralwerte längs gewisser Mannigfaltigkeiten," Ber. Verh. Sächs. Akad. Wiss. Leipzig, Math.-Nat. Kl. 69, 262-277 (1917).
- [2] Hounsfield, G. N., "A method of and apparatus for examination of a body by radiation such as X- or gamma radiation," UK Patent 1283915 (1972).
- [3] Hovland, H., "Tomographic scanning imager," Opt. Express 17(14), 11371-11387 (2009).
- [4] Hovland, H., "Construction and demonstration of a multispectral tomographic scanning imager (TOSCA)," Opt. Express 17(14), 11371-11387 (2009).
- [5] Hovland, H., "Tomographic scanning imaging seeker," Proc. SPIE 5430, 76-85 (2004).
- [6] Hovland, H., "Specialized tomographic scanning imaging seeker," Proc. SPIE 5778, 725-738 (2005).
- [7] Hovland, H., "Optimization of the tomographic scanning (TOSCA) imager," Proc. SPIE 6569, 65690I (2007).
- [8] Kak, A., Slaney, M., [Principles of computerized tomographic imaging], IEEE Press, New York, 70-71 (1988).
- [9] Hsieh, J., [Computed tomography principles, design, artefacts, and recent advances], SPIE Optical Engineering Press, Bellingham, WA, 167-240 (2003).
- [10] Bracewell, R. H., Riddle, A. C., "Inversion of fan beam scans in radio astronomy," Astrophys. Journ. 150, 427-434 (1967).
- [11] Mourolis, P., Green, R. O., Chrien, T. G., "Design of pushbroom imaging spectrometers for optimum recovery of spectroscopic and spatial information," Appl. Opt. 39, 2210-2220 (2000).